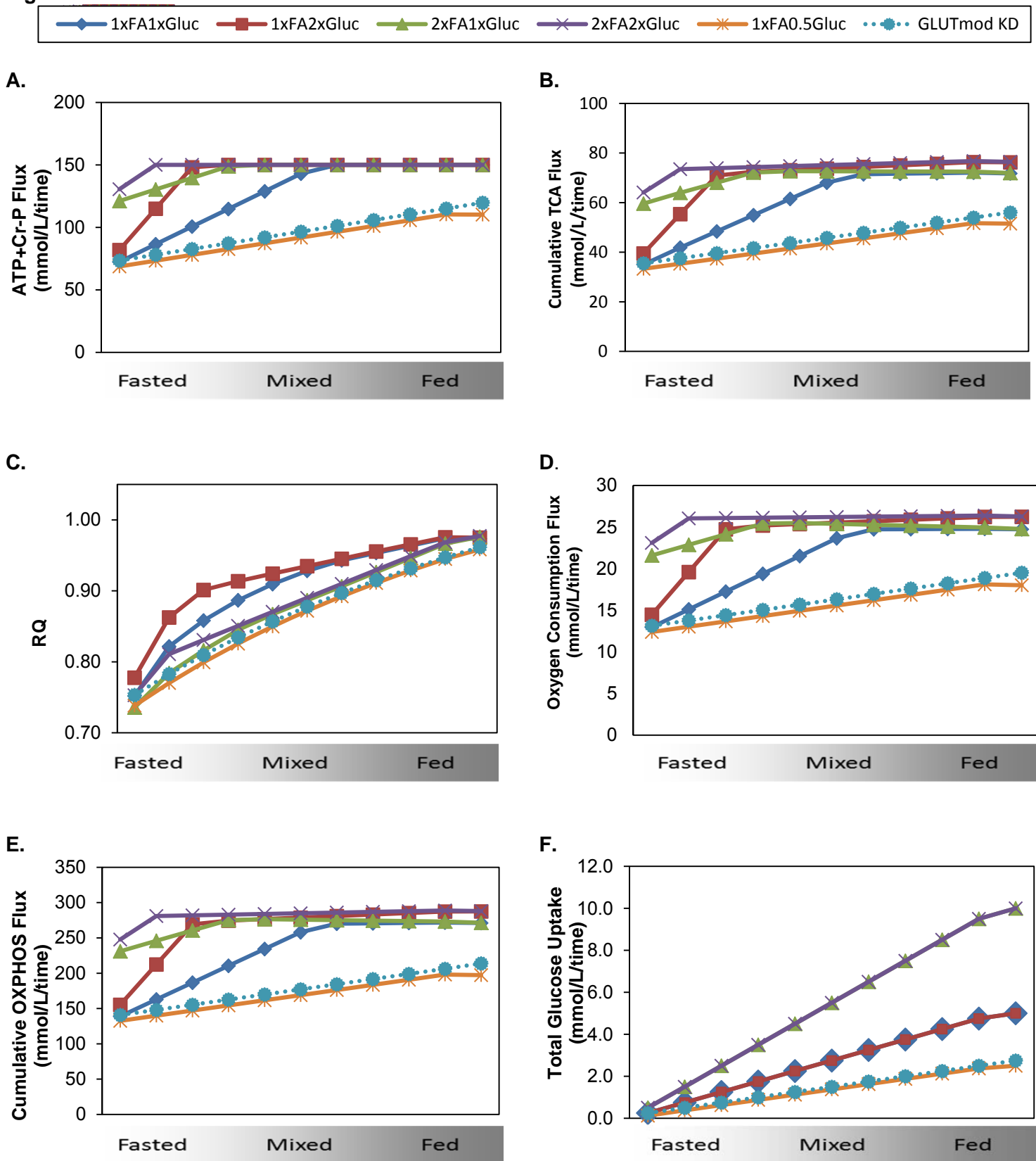


Figure S1

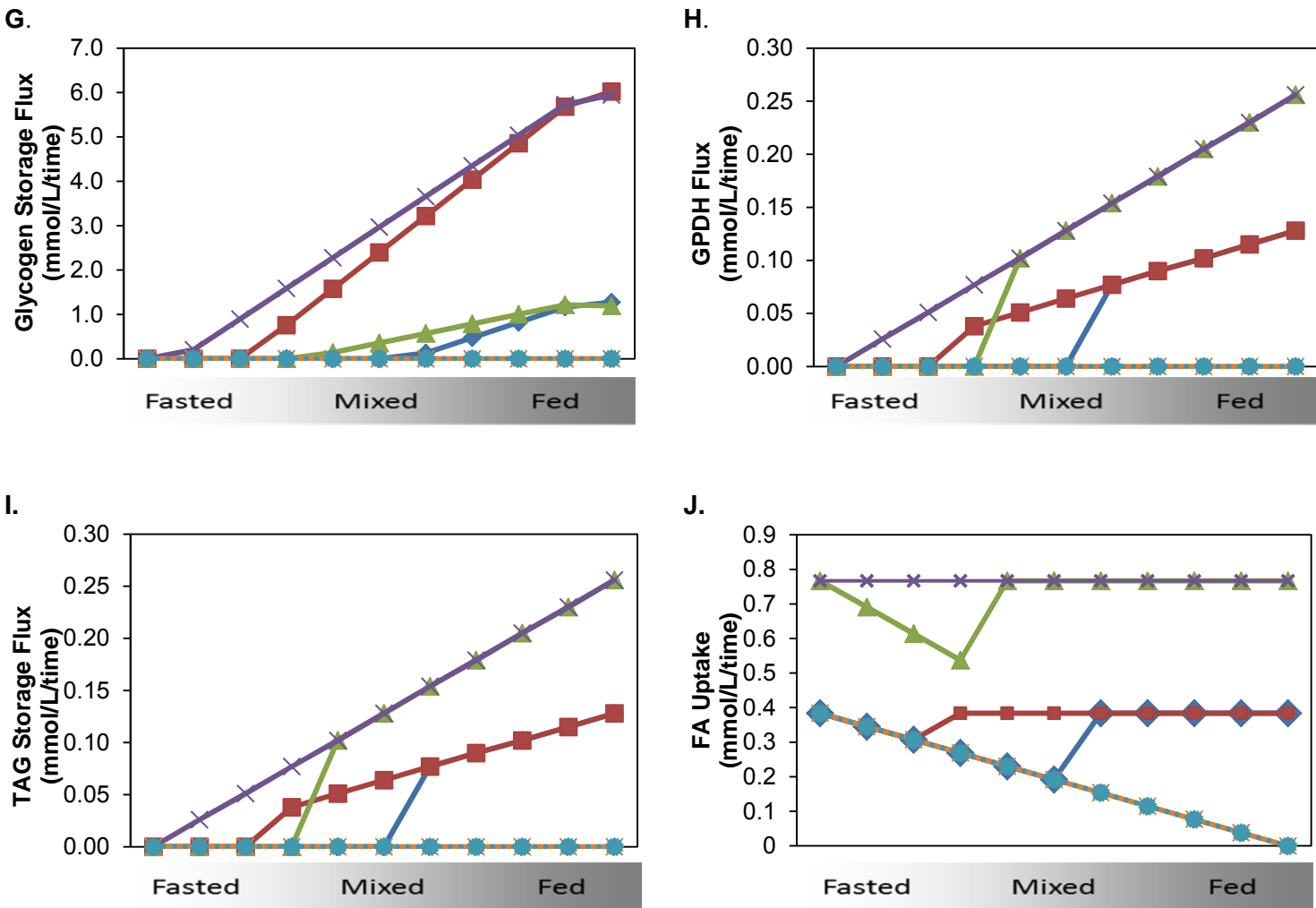
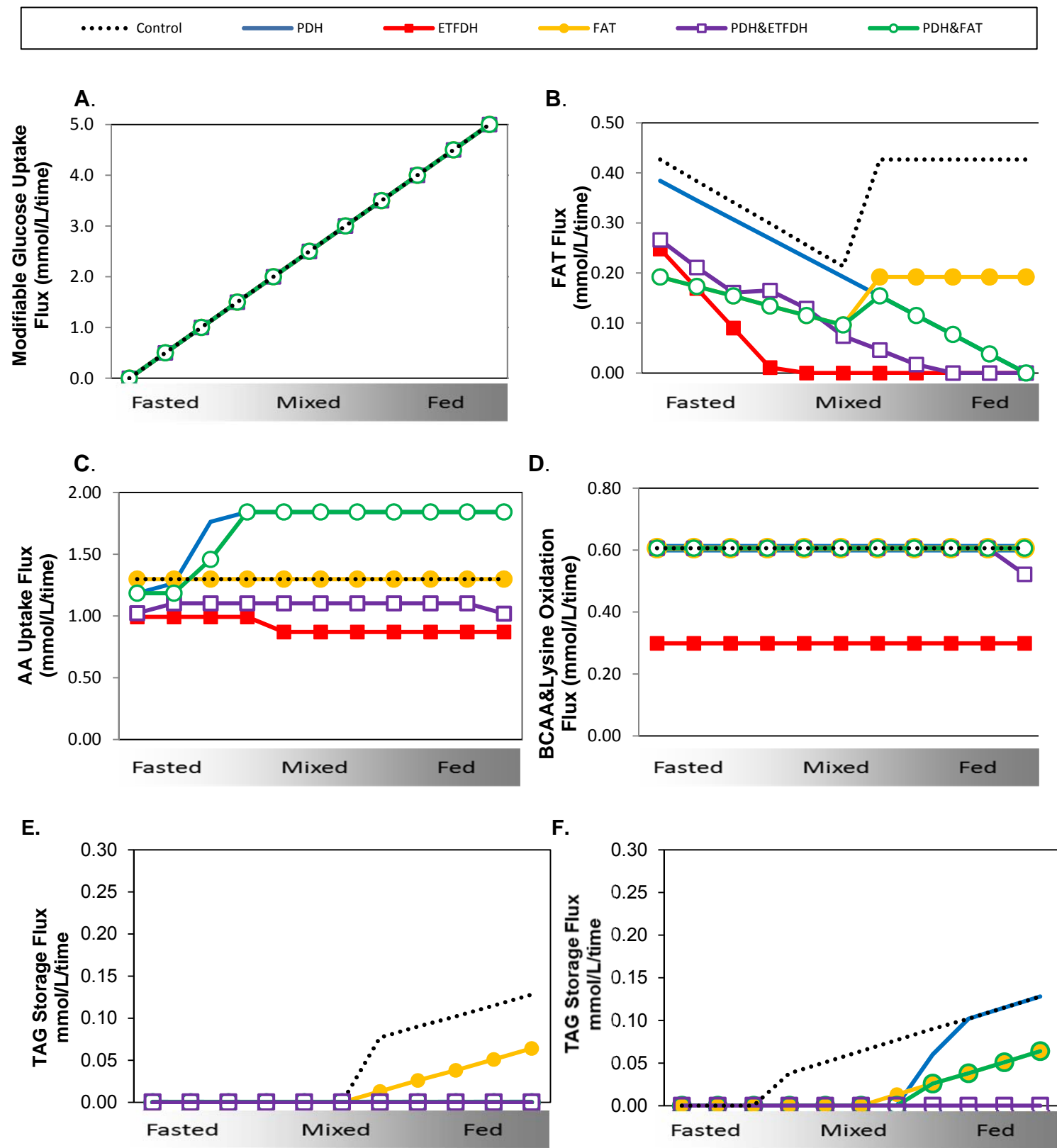
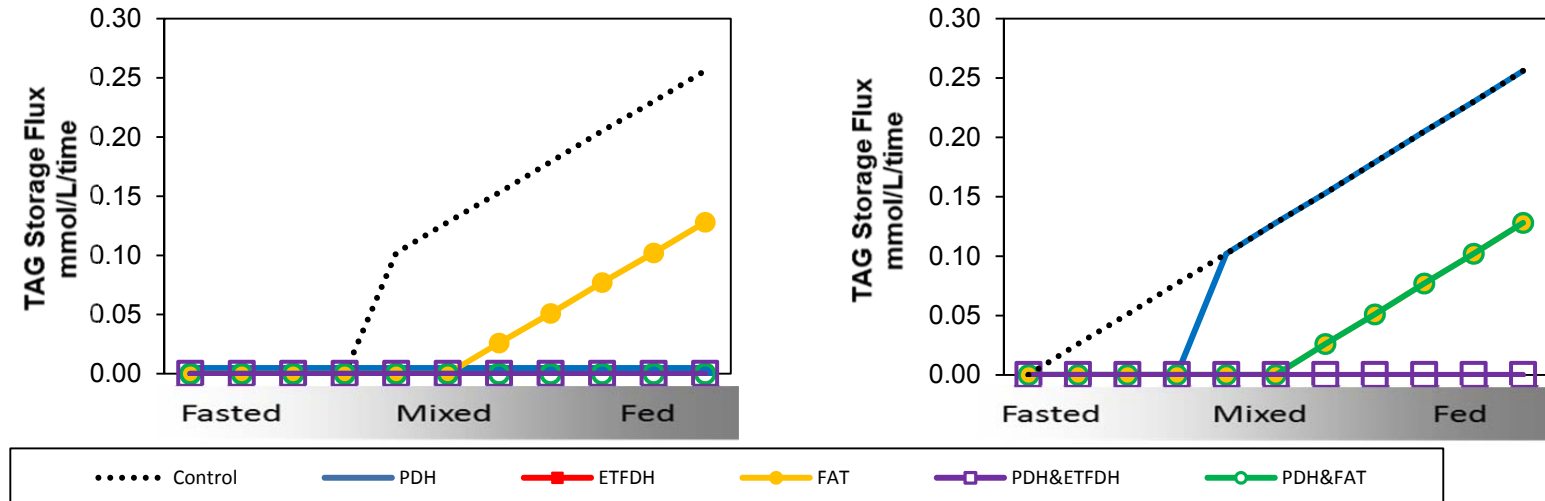


Figure S1. Predicted fluxes through pathways and substrate uptake, production, and release. Chart shows the flux in mmol/L/time on the Y-axis. The x-axis shows the flux at the discrete points from our defined fasting to fed states, as defined by conversely constraining the flux through CPT1 and modifiable glucose uptake from 0-100% of the maximum flux. The different nutrient states, defined in the text, are indicated by different colored lines and symbols: 1xFA/1xGluc (blue/diamonds), 1xFA/2xGluc (red/boxes), 2xFA/1xGluc (green/triangle), 2xFA/2xGluc (purple/x), 1xFA/0.5xGluc (orange/*), and 1xFA/1xGluc GLUT_{mod} knockdown (aqua/dashed/circles). (A) Predicted ATP+Cr-P production, constrained to a maximum of 150 mmol/time (ATP limit 33.3 mmol/time; Cr-P limit 116.7 mmol/time). (B) Predicted cumulative flux through the TCA cycle, including citrate synthase, aconitase, isocitrate dehydrogenase-2, α -ketoglutarate dehydrogenase, succinyl coenzyme-A synthetase, succinate dehydrogenase, fumarase, and malate dehydrogenase-2 reactions. (C) Predicted respiratory quotient (RQ). (D) Predicted oxygen consumption. (E) Cumulative flux through electron transport chain (complexes I-V). (F) Total glucose uptake (basal + modifiable). (G) Predicted glycogen storage. (H) Glucose oxidation, as measured by flux through glycerol-3-phosphate dehydrogenase (GPDH) reaction. (I) Predicted TAG storage. (J) Fatty acid uptake.

Figure S2.



G.



H.

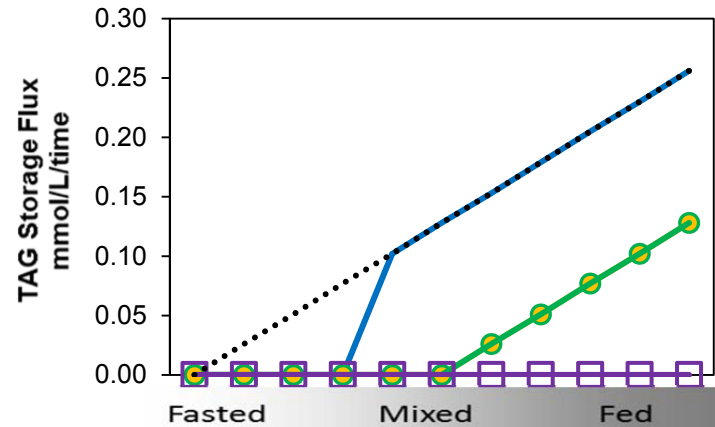


Figure S2. Combined knockdown of PDH and ETFDH or FAT predicts effects on amino acid metabolism and fatty acid metabolism. (A) The modifiable glucose uptake is not altered by any of the specified KDs. (B) KDs in multiple reactions predicts reduction in fatty acid uptake. (C) PDH and the combined PDH&FAT KDs increase amino acid uptake while ETFDH and the combined PDH&ETFDH KDs reduce amino acid uptake. (D) ETFDH KD reduces BCAA and lysine oxidation. TAG storage in the following nutrient states: (E) 1xFA1xGluc. (F) 1xFA2xGluc. (G) 2xFA1xGluc. (H) 2xFA2xGluc.

Figure S3.

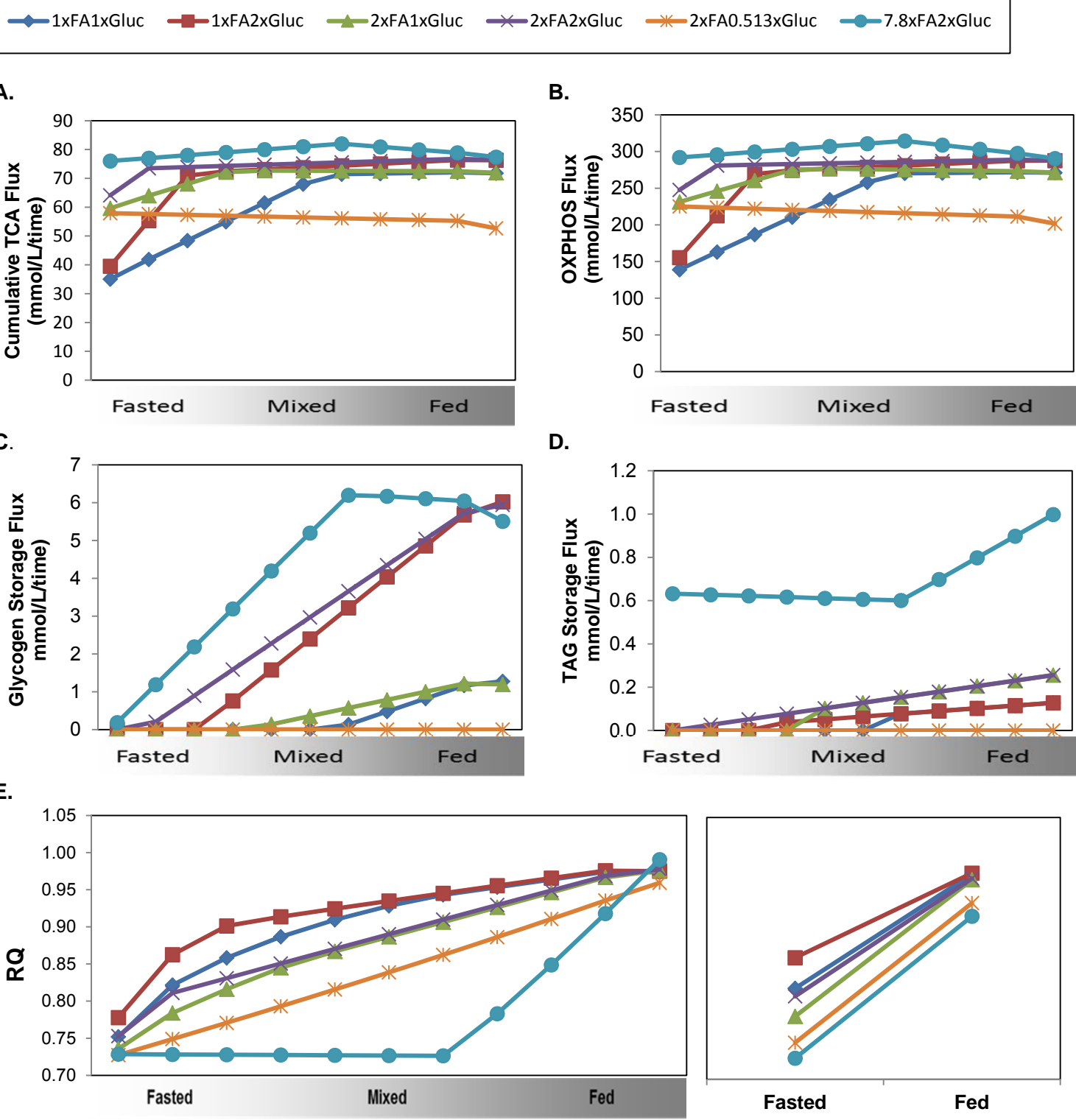


Figure S3. Predicted fluxes through pathways and substrate uptake, production, and release in different nutrient conditions. Flux in mmol/L/time (Y-axis) is assessed in fasting to fed states, as defined by conversely constraining the flux through CPT1 and modifiable glucose uptake from 0-100% of the maximum flux. The different nutrient states, defined in the text, are indicated by different colored lines and symbols: 1xFA1xGluc (blue/diamonds), 1xFA2xGluc (red/boxes), 2xFA1xGluc (green/triangle), 2xFA2xGluc (purple/x), 2xFA0.513xGluc (orange/star), and 7.8xFA2xGluc (aqua/circle). (A) Predicted cumulative flux through the TCA cycle, including citrate synthase, aconitase, isocitrate dehydrogenase-2, α -ketoglutarate dehydrogenase, succinyl coenzyme-A synthetase, succinate dehydrogenase, fumarase, and malate dehydrogenase-2 reactions. (B) OXPHOS (complexes I-V). (C) Predicted glycogen storage. (D) Predicted TAG storage. (E) Predicted respiratory quotient (RQ).

Table S1. Basal concentrations used as maximal uptake fluxes in the Flux Balance Model.

Metabolite	Concentration (mmol/L) ¹
Glucose*	5.00
Palmitate*	0.3875
Arginine	0.080 \pm 20
Histidine	0.082 \pm 10
Isoleucine	0.062 \pm 14
Leucine	0.123 \pm 25
Lysine	0.188 \pm 32
Methionine	0.025 \pm 04
Phenylalanine	0.057 \pm 09
Threonine	0.140 \pm 33
Tryptophan	0.044 \pm 07
Valine	0.233 \pm 43
Alanine	0.333 \pm 74
Asparagine	0.041 \pm 10
Aspartate	0.003 \pm 01
Cysteine	0.052 \pm 11
Glutamate	0.024 \pm 15
Glutamine	0.586 \pm 84
Glycine	0.230 \pm 52
Proline	0.168 \pm 60
Serine	0.114 \pm 19
Tyrosine	0.590 \pm 12

1. Cynober et al (2002), and MacLaren (2000), except:

*Glucose and Fatty Acid: based on internal data collected in the Patti Lab

Table S2A. KDs in 1xFA-1xGluc causing significant reductions in ATP+Cr-P production.

Table S2B. KDs in 1xFA-1xGluc causing significant reductions in cumulative TCA flux.

Table S2C. KDs in 1xFA-1xGluc causing significant reductions in metabolic flexibility as measured by RQ differences.

EC Number	Reaction	Score	p
1.2.4.1	PyrSynth-pdh	-0.09	0.01
n/a	Ex_pal	-0.03	0.43
n/a	FAT-CD36	-0.03	0.43
6.2.1.3	ACSL/PalTK	-0.03	0.43
n/a	Glu-AspEx	-0.01	0.71
2.6.1.1	ASTM	-0.01	0.71
n/a	ASTC	-0.01	0.73
n/a	NEAA_asp	0.00	0.88

Table S2D. KDs in 2xFAs-2xGluc causing significant reductions in ATP+Cr-P production.

Table S2E. KDs in 2xFA-2xGluc causing significant reductions in cumulative TCA flux.

Table S2F. KDs in 2xFA-2xGluc causing significant reductions in metabolic flexibility as measured by RQ differences.

EC Number	Reaction	Score	p
1.2.4.1	PyrSynth-pdh	-0.22	0.00044
n/a	Ex_pal	-0.046	0.21
n/a	FAT-CD36	-0.046	0.21
6.2.1.3	ACSL/PalTK	-0.046	0.21

Table S2G. Top KDs causing reduced metabolic flexibility in the 2xFA-2xGluc increased nutrient condition. For metabolic flexibility, data indicate cumulative difference in RQ (Eq. 8 in text). For each KD, data indicate ratio of KD compared to control (Eq. 6 and 7 in text).

KD Reaction	EC Number	Met. Flex	ATP+Cr-P Production			Cumulative TCA Flux		
			ΔRQ	Fasted	Mixed	Fed	Fasted	Mixed
PDH	1.2.4.1	0.22	0.96	0.78	0.80	0.96	0.90	0.82
FAT-CD36	n/a	0.05	0.81	1.00	1.00	0.74	1.00	1.00
ACSL/PalTK	6.2.1.3	0	0.81	1.00	1.00	0.74	1.00	1.00

Table S3A. KDs with scores less than 1 in each of the pathways contributing to pathway enrichment in the 1xFA-1xGluc nutrient condition: **reduced ATP+Cr-P production.** No pathways were enriched in the fed condition.

BCAA	
Fasted	Mix
SucDeh-II	SucDeh-II
CitSynth	CitSynth
ButyrlCoADeh	ASTM
DLDH	DLDH
AcyICoAAT-But	PCCB
ASTM	MCEE
EnoCoADeh-But	AcylCoAAT-But
3HA-CoADeh-But	ButyrlCoADeh
PCCB	BCAT2-val
MCEE	BCKDHB-val
BCAT2-val	BCKADE2-val
BCKDHB-val	ACADSB
BCKADE2-val	ECHS1
ACADSB	HIBCH
ECHS1	HIBADH
HIBCH	ALDH6A1
HIBADH	ECHS1
ALDH6A1	MT_val
ECHS1	MUT
MT_val	EnoCoADeh-But
MUT	3HA-CoADeh-But
BCAT2-leu	BCAT2-leu
BCKDHB-leu	BCKDHB-leu
BCKADE2-leu	BCKADE2-leu
IVD	IVD
MCC1-MCC2	MCC1-MCC2
MGCA	MGCA
HMGCL	HMGCL
OXCT	OXCT
MT_leu	MT_leu
ECHS1	ECHS1
BCKDHB-ile	BCKDHB-ile
BCKADE2-ile	BCKADE2-ile
ECHS1	ECHS1
HSD17B10_	HSD17B10_
ACAT1	ACAT1
MT_ile	MT_ile
ALT	ALT

Butanoate	
Fasted	Mix
SucDeh-II	SucDeh-II
Fum	Fum
CitSynth	CitSynth
Acon	Acon
ButyrlCoADeh	ASTM
AcylCoAAT-But	AcylCoAAT-But
ASTM	ButyrlCoADeh
EnoCoADeh-But	ECHS1
3HA-CoADeh-But	EnoCoADeh-But
ECHS1	3HA-CoADeh-But
HMGCL	HMGCL
OXCT	OXCT
ECHS1	ECHS1
ACAT1	ACAT1

Lysine	
Fasted	Mix
AKGDeh	AKGDeh
AcylCoAAT-But	AcylCoAAT-But
EnoCoADeh-But	ECHS1
3HA-CoADeh-But	EnoCoADeh-But
ECHS1	3HA-CoADeh-But
ECHS1	ECHS1
ACAT1	ACAT1
AASS	AASS
AASS	AASS
aAASADeh	aAASADeh
KATII	KATII
GCDH	GCDH
lysdeg	lysdeg
MT_ly	MT_ly

Table S3B. KDs with scores less than 1 in each of the pathways contributing to pathway enrichment in the 1xFA-1xGluc nutrient condition: **cumulative TCA Flux**. No pathways were enriched in the fed condition.

BCAA	
Fasted	Mix
ASTM	ASTM
SucDeh-II	SucDeh-II
AcylCoAAT-But	AcylCoAAT-But
ButyrlCoADeh	ButyrlCoADeh
EnoCoADeh-But	EnoCoADeh-But
3HA-CoADeh-But	3HA-CoADeh-But
CitSynth	CitSynth
DLDH	DLDH
PCCB	PCCB
MCEE	MCEE
BCAT2-leu	BCAT2-leu
BCKDHB-leu	BCKDHB-leu
BCKADE2-leu	BCKADE2-leu
IVD	IVD
MCC1-MCC2	MCC1-MCC2
MGCA	MGCA
HMGCL	HMGCL
OXCT	OXCT
MT_leu	MT_leu
ALT	ALT
BCAT2-val	BCAT2-val
BCKDHB-val	BCKDHB-val
BCKADE2-val	BCKADE2-val
ACADSB	ACADSB
ECHS1	ECHS1
HIBCH	HIBCH
HIBADH	HIBADH
ALDH6A1	ALDH6A1
ECHS1	ECHS1
MT_val	MT_val
ECHS1	ECHS1
BCKDHB-ile	BCKDHB-ile
BCKADE2-ile	BCKADE2-ile
ECHS1	ECHS1
HSD17B10_	HSD17B10_
ACAT1	ACAT1
MT_ile	MT_ile

Butanoate	
Fasted	Mix
ASTM	ASTM
SucDeh-II	SucDeh-II
Fum	Fum
AcylCoAAT-But	AcylCoAAT-But
ButyrlCoADeh	ButyrlCoADeh
EnoCoADeh-But	EnoCoADeh-But
3HA-CoADeh-But	3HA-CoADeh-But
CitSynth	CitSynth
Acon	Acon
HMGCL	HMGCL
OXCT	OXCT
ECHS1	ECHS1
ECHS1	ECHS1
ACAT1	ACAT1

Lysine	
Fasted	Mix
AKGDeh	AKGDeh
AcylCoAAT-But	AcylCoAAT-But
EnoCoADeh-But	EnoCoADeh-But
3HA-CoADeh-But	3HA-CoADeh-But
AASS	AASS
AASS	AASS
aASAdeh	aASAdeh
KATII	KATII
GCDH	GCDH
lysdeg	lysdeg
MT_lys	MT_lys
ECHS1	ECHS1
ECHS1	ECHS1
ACAT1	ACAT1

Propanoate	
Fasted	Mix
ASTM	ASTM
Fum	Fum
PCCB	PCCB
MCEE	MCEE
ECHS1	ECHS1
HIBCH	HIBCH
ALDH6A1	ALDH6A1
ECHS1	ECHS1
ECHS1	ECHS1
ECHS1	ECHS1
ACAT1	ACAT1

FAD metabolism	
Fasted	Mix
ETFDH	
SucDeh-II	
AcylCoADeh	
AcylCoADeh-14-c	
AcylCoADeh-12-c	
AcylCoADeh-10-c	
AcylCoADeh-8-c	
AcylCoADeh-6-c	
ButyrlCoADeh	
IVD	
ACADSB	

Tryptophan	
Fasted	Mix
AKGDeh	AKGDeh
AcylCoAAT-But	AcylCoAAT-But
EnoCoADeh-But	EnoCoADeh-But
3HA-CoADeh-But	3HA-CoADeh-But
GCDH	GCDH
ALT	ALT
ECHS1	ECHS1
ECHS1	ECHS1
ACAT1	ACAT1

TCA Cycle	
Fasted	Mix
MalDehM	
AKGDeh	
SucDeh-II	
Fum	
MCT	
CitSynth	
Acon	
DLDH	

Table S3C. KDs with scores less than 0 in each of the pathways contributing to pathway enrichment in the 1xFA-1xGluc nutrient condition: ***metabolic inflexibility***.

Glycerophospholipid metabolism	Lysine metabolism	NADH Shuttle
G3PDechC	EnoCoADeh-But	3HA-CoADeh
GPAT4	3HA-CoADeh-But	3HA-CoADeh-14c
ABHD5	AASS	3HA-CoADeh-12c
DAGZ-DAGK6	AASS	3HA-CoADeh-10c
TAG Storage	aAASADeh	PGD
	KATII	3HA-CoADeh-8c
	GCDH	GluDeh
	LysDeh	PYRCR1
	Lys transport	MalDehC
		G3PDehC
		AASS
		AASS
		aAASADeh
		lysdeg

Table S3D. Pathways enriched in causing IR phenotypes ($p < 0.05$; $Q < 0.25$).

ATP + Cr-P Production	Cumulative TCA Flux	Metabolic Inflexibility
BCAA (fasted and mixed) Butanoate (fasted and mixed) Lysine (fasted and mixed)	BCAA (fasted and mixed) Butanoate (fasted and mixed) Lysine (fasted and mixed) Propanoate (fasted and mixed) TCA Cycle (fasted only) Tryptophan (fasted and mixed) FAD metabolism (fasted only)	Glycerophospholipid Lysine NADH shuttle

Table S3E. KDs with scores less than 1 in each of the pathways contributing to pathway enrichment in the 2xFA-2xGluc nutrient condition: **reduced ATP+Cr-P production**. No pathways were enriched in the fed condition.

Fatty Acid Metabolism	
Fasted	Mix
SucDeh-II	Not enriched
CPT1B-CHKL	
CPT2	
AcyCoADeh	
EnoCoADeh	
3HA-CoADeh	
AcyCoAAT	
CPT1B-CHKL	
CPT2	
ACSL/PalTK	
AcyCoADeh-14-c	
EnoCoADeh-14c	
3HA-CoADeh-14c	
AcyCoAAT-14c	
AcyCoADeh-12-c	
EnoCoADeh-12c	
3HA-CoADeh-12c	
AcyCoAAT-12c	
AcyCoADeh-10-c	
EnoCoADeh-10c	
3HA-CoADeh-10c	
AcyCoAAT-10c	
AcyCoADeh-8-c	
EnoCoADeh-8c	
3HA-CoADeh-8c	
AcyCoAAT-8c	
AcyCoADeh-6-c	
EnoCoADeh-6c	
3HA-CoADeh-6c	
AcyCoAAT-6c	

NADH Shuttle	
Fasted	Mix
MalDehM	MalDehM
NADHDeh-I	NADHDeh-I
AKGDeh	D3PDeh
3HA-CoADeh	MalDehC
3HA-CoADeh-14c	AKGDeh
D3PDeh	
3HA-CoADeh-12c	
MalDehC	
3HA-CoADeh-10c	
3HA-CoADeh-8c	
3HA-CoADeh-6c	

TCA Cycle	
Fasted	Mix
MalDehM	MalDehM
SucDeh-II	MCT
Fum	SucDeh-II
AKGDeh	Fum
CitSynth	AKGDeh
Acon	
MCT	

Glycolysis	
Fasted	Mix
D3PDeh	Not enriched
PGK	
Hex	
TPI	
PFK	
Ald	

OXPHOS	
Fasted	Mix
ATPSynth-V	ATPSynth-V
UCytC-III	UCytC-III
CytCO-IV	CytCO-IV
NADHDeh-I	NADHDeh-I
SucDeh-II	SucDeh-II

Table S3F. KDs with scores less than 1 in each of the pathways contributing to pathway enrichment in the 2xFA-2xGluc nutrient condition: **cumulative TCA Flux**. No pathways were enriched in the fed condition.

Glycerolipid/glycerophospholipid	
Fasted	Mix
Hex	Hex
Fum	Fum
GPAT4	GPAT4
ABHD5	ABHD5
DAGZ-DAGK6	DAGZ-DAGK6
DGAT1	DGAT1
St_TAG	St_TAG
G3PDehC	G3PDehC
GPAT4	GPAT4
ABHD5	ABHD5
DAGZ-DAGK6	DAGZ-DAGK6
St_TAG	St_TAG

NADH Shuttle	
Fasted	Mix
MalDehM	MalDehM
NADHDeh-I	NADHDeh-I
MalDehC	MalDehC
D3PDeh	D3PDeh
AKGDeh	AKGDeh
AASS	AASS
AASS	AASS
aAASADeh	aAASADeh
lysdeg	lysdeg
DLDH	DLDH
G3PDehC	G3PDehC

Glycolysis	
Fasted	Mix
D3PDeh	D3PDeh
PGK	PGK
Hex	Hex
TPI	TPI
PFK	PFK
Ald	Ald
PGM1	PGM1
DLDH	DLDH
PGI	PGI

Lysine	
Fasted	Mix
AKGDeh	Not enriched
AASS	
AASS	
aAASADeh	
KATII	
GCDH	
lysdeg	
MT_lys	

OXPHOS	
Fasted	Mix
NADHDeh-I	NADHDeh-I
ATPSynth-V	ATPSynth-V
UCytC-III	UCytC-III
CytCO-IV	CytCO-IV
SucDeh-II	SucDeh-II

Table S3G. KDs with scores less than 0 in each of the pathways contributing to pathway enrichment in the 2xFA-2xGluc nutrient condition: ***metabolic inflexibility***.

Glycerophospholipid metabolism
G3PDehC
GPAT4
ABHD5
DAGZ-DAGK6
St_TAG

Table S3H. Pathways enriched in causing IR phenotypes ($p < 0.05$; $Q < 0.25$, except otherwise indicated) in the 2xFA-2xGluc increased nutrient condition.

ATP + Cr-P Production	Cumulative TCA Flux	Metabolic Inflexibility
Fatty Acid Metabolism (Fasted only)	Glycerolipid/glycerophospholipid (fasted and mixed)	Glycerophospholipid ($p < 0.05$; $Q = 0.73$)
Glycolysis (fasted only)	Glycolysis (fasted and mixed)	
OXPHOS (fasted and mixed)	Lysine (fasted only)	
TCA Cycle (fasted and mixed)	OXPHOS (fasted and mixed)	
NADH Shuttle (fasted and mixed)	NADH Shuttle (fasted and mixed)	

Table S4A. Summary of scores for the top KDs causing reduced metabolic flexibility in basal nutrient condition (1xFA-1xGluc). For metabolic flexibility, data indicate cumulative difference in RQ (**Eq. 8** in text). For each KD, data indicate ratio of KD compared to control (**Eq. 6** and **7** in text).

KD Reactions	EC Numbers	Met. Flex	ATP+Cr-P Production			Cumulative TCA Flux		
		ΔRQ	Fasted	Mixed	Fed	Fasted	Mixed	Fed
PDH & ETFDH	1.2.4.1 & 1.5.5.1	0.21	0.58	0.61	0.70	0.55	0.56	0.61
PDH & FAT-CD36	1.2.4.1 & n/a	0.16	0.69	0.71	0.80	0.65	0.68	0.73
PDH & ASN Synth	1.2.4.1 & 2.7.2.11	0.15	0.94	0.76	0.78	0.93	0.73	0.69
FAT-CD36 & MCT	n/a & n/a	0.29	0.68	0.66	0.75	0.61	0.60	0.66
AST & FAT-CD36	2.6.1.1 & n/a	0.10	0.73	0.65	0.68	0.69	0.62	0.63
AST & ETFDH	2.6.1.1 & 1.5.5.1	0.06	0.60	0.58	0.61	0.58	0.59	0.58

Table S4B. Summary of scores for the top **DOUBLE** KDs in 2xFA-2xGluc increased nutrient condition. For metabolic flexibility, data indicate cumulative difference in RQ (**Eq. 8** in text). For each KD, data indicate ratio of KD compared to control (**Eq. 6** and **7** in text).

KD Reactions	EC Numbers	Met. Flex	ATP+Cr-P Production			Cumulative TCA Flux		
		ΔRQ	Fasted	Mixed	Fed	Fasted	Mixed	Fed
PDH & ETFDH	1.2.4.1 & 1.5.5.1	0.32	0.58	0.78	0.98	0.53	0.63	0.73
PDH & FAT-D36	1.2.4.1 & n/a	0.37	0.72	1.00	1.00	0.66	0.90	0.82
PDH & ASN Synth	1.2.4.1 & 2.7.2.11	0.24	0.96	1.00	1.00	0.92	0.86	0.79
FAT-CD36 & MCT	n/a & n/a	0.41	0.68	0.98	1.00	0.60	0.83	0.77
AST & FAT-CD36	2.6.1.1 & n/a	0.15	0.71	0.85	0.79	0.65	0.77	0.64
AST & ETFDH	2.6.1.1 & 1.5.5.1	0.02	0.57	0.64	0.70	0.55	0.62	0.58

Table S5. Human microarray expression data for ETF and PDH subunits in muscle biopsy samples from insulin sensitive (IS) individuals vs. patients with type 2 diabetes (T2D), and correlations with insulin sensitivity ($\log_2 S_I$). One tailed t tests were used to derive p values.

Probeset	Gene	Fold Change, T2D-IS	P, IS vs. T2D	Correlation with Log2 SI	P for Correlation
201573_s_at	ETF1	-1.13	0.09	0.24	0.05
201574_at	ETF1	1.09	0.87	-0.20	0.92
201931_at	ETFA	-1.09	0.16	0.03	0.42
202942_at	ETFB	-1.13	0.13	-0.01	0.52
240933_at	ETFB	-1.69	0.04	0.11	0.23
205530_at	ETFDH	-1.14	0.12	-0.05	0.63
33494_at	ETFDH	-1.21	0.06	-0.04	0.60
1555864_s_at	PDHA1	-1.29	0.01	0.25	0.04
200980_s_at	PDHA1	-1.21	0.03	0.19	0.10
242581_at	PDHA1	-1.13	0.34	0.23	0.06
214518_at	PDHA2	1.59	0.95	-0.27	0.97
208911_s_at	PDHB	-1.3	0.00	0.27	0.03
211023_at	PDHB	-1.28	0.01	0.28	0.03
203067_at	PDHX	-1.21	0.02	0.23	0.06
206686_at	PDK1	1.03	0.46	0.01	0.52
226452_at	PDK1	-1.23	0.98	0.41	1.00
202590_s_at	PDK2	1.15	0.25	-0.12	0.21
213724_s_at	PDK2	1.09	0.34	-0.03	0.42
206347_at	PDK3	1.16	0.27	0.00	0.50
206348_s_at	PDK3	1.23	0.10	-0.35	0.01
221957_at	PDK3	-1.01	0.52	-0.01	0.46
228959_at	PDK3	1.16	0.07	0.03	0.57
230085_at	PDK3	-1.28	0.82	0.19	0.90
1562321_at	PDK4	3.98	0.01	-0.24	0.05
205960_at	PDK4	3.54	0.00	-0.32	0.01
225207_at	PDK4	2.68	0.00	-0.31	0.02

Supplemental Experimental Procedures

Model

The muscle flux balance model developed here integrates the model of the mitochondrion developed by Palsson and colleagues (Ramakrishna et al., 2001), but adds critical elements of muscle-specific metabolism, including amino acid metabolism, protein synthesis, fatty acid oxidation and synthesis, and pentose phosphate metabolism. Many techniques have been used to optimize prediction accuracy (Segre et al., 2002; Oberhardt et al., 2009). Here, we used a simple approach utilizing MatLab as the software package (Version 7.11.0584 (R2010b) 64 bit). The optimization software is the open-source GLPK MatLab interface (Version 2.4): ©2001-2007, Nicolo' Giorgetti, which uses linear programming to optimize a specified objective function; all default settings were used.

Choosing the Objective Function

We make the assumption that the main objectives of resting muscle tissue (either during the fasting or fed states) is to maximize a complex objective function combining storage of energy in the forms of high-energy phosphates (ATP+Cr-P), glycogen, and TAG for energy needs during subsequent contraction. While ATP and Cr-P are independent reactions within the model, we summed these substrate molecules as sources of high-energy phosphate production and weighted the sum of ATP+Cr-P production to be twice that of the other energy storage molecules. For ATP production, we maximize a reaction within the model describing ATP storage (**Eq. 1**), encompassing both aerobic and non-aerobic ATP production.

Eq.1:

$$ATP \text{ production} =$$

$$\Sigma(\text{aerobic ATP production}) + \Sigma(\text{nonaerobic ATP Production})$$

For Cr-P, glycogen, and TAG, we maximize flux through reactions describing storage for each substrate. Since muscle tissue can only store a finite amount of ATP+Cr-P, we set an upper limit of 33.3 and 116.7 mmol/time for ATP+Cr-P production/storage, respectively, based on prior data demonstrating an 3.5-fold ratio of Cr-P to ATP content (Sleigh et al., 2011; Gray et al., 2008). Together with our initial input values (**Supplemental Table S1**), we set these limits (paralleling rates and quantity at which ATP and Cr-P are synthesized *in vivo*) in order to allow extra substrate to be stored in glycogen, triglycerides, or muscle protein (**Figure 1B**).

Modeling the Dynamics of Normal Metabolism

Flux balance analysis (FBA) typically models metabolism in a steady state, but we wished to simulate the metabolic transitions between fasting and fed conditions. To this aim, we reciprocally modulate lipid oxidation and glucose uptake. Given that lipid utilization is maximal in the fasting state and reduced in the fed state, we first modulated lipid oxidation by limiting CPT1—the enzyme controlling fatty acid uptake into mitochondria for subsequent oxidation—from a maximum activity of 100% (fasted) to a minimum of 0% (fed) through a progressive stepwise reduction in activity (**Figure 1B**). We simultaneously modeled glucose uptake in two distinct components: basal and modifiable. First, we estimated basal glucose uptake (GU_{bas}) to be 5% of the glucose

concentration in plasma, constant across the fasted to fed transition (Kraegen et al., 1993; Kelley et al., 1993; Kelley et al., 1992; Mandarino et al., 1993). In addition, we modeled a modifiable glucose uptake (GU_{mod}) by adjusting the maximal glucose uptake from 0% to 100% of the concentration found in plasma (**Figure 1B**). We defined three steady states across this continuum: fasted (90% CPT1, 10% GU_{mod}), mixed (50% CPT1, 50% GU_{mod}), and fed (10% CPT1, 90% GU_{mod}) (**Figure 1B**). These steady states were used to examine the impact of the metabolic condition on *in silico* KDs (see **In Silico Knockdowns** below). In all conditions, we allow free uptake of fatty acids and amino acids up to the values found in plasma in healthy fasting individuals (Jin et al., 2011; Cynober, 2002).

Nutrient Conditions

Since prevailing nutrient conditions are a key determinant of cellular metabolism, we assigned basal (1x) concentrations of extracellular glucose, fatty acids, and amino acids from values in healthy subjects (Jin et al., 2011; Cynober, 2002) (**Table S1**). To examine the impact of increased substrate availability, we also created three additional nutrient conditions, yielding increased fatty acids and glucose independently (2xFA-1xGluc or 1xFA-2xGluc) and in combination (2XFA-2XGluc). We also examined the impact of reduced glucose uptake, as observed in insulin resistance, by reducing either glucose availability (0.5xGluc) or reducing the modifiable glucose uptake to 50% of its flux across the fasting to fed transition (GLUTmod KD).

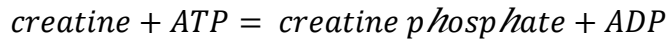
***In Silico* Knockdowns**

We simulated knockdowns (KDs) of each reaction R by constraining the flux for reaction R to 50% its normal, optimal value for each of the 3 defined states (fasted, mixed, and fed). After constraining the reaction to this new, reduced value, we re-optimized the model to obtain another set of fluxes (**Figure 2A**) and compared metabolic phenotypes to the basal (no knockdown) condition.

Modeling Insulin Resistance Phenotypes

We wish to identify which metabolic reactions or networks may perturb muscle metabolism sufficiently to yield metabolic phenotypes observed in insulin resistance. Given that our model does not incorporate insulin signaling, we used three key metabolic phenotypes characteristic of human insulin resistance as a proxy for insulin resistance: (1) reduced ATP+Cr-P production (Petersen et al., 2004; Petersen et al., 2005), (2) reduced flux through TCA cycle (Befroy et al., 2007; Simoneau and Kelley, 1997), and (3) reduced metabolic flexibility (Kelley and Mandarino, 2000). In order to determine the effect of *in silico* KDs on these phenotypes, we define them mathematically for our model. For ATP production, we monitor a reaction within the model describing ATP storage (**Eq. 1**), encompassing both aerobic and non-aerobic ATP production. For Cr-P, we examine the creatine kinase reaction (**Eq. 2**). To quantify TCA cycle activity, we sum the fluxes through all reactions within the TCA cycle (**Eq. 3**).

Eq. 2:



Eq. 3:

$$\begin{aligned}\Sigma(\text{TCA Flux}) &= \text{citrate synthase} + \text{aconitase} + \text{isocitrate dehydrogenase 2} \\ &+ \alpha\text{-ketoglutarate dehydrogenase} \\ &+ \text{succinyl Coenzyme A synthetase} \\ &+ \text{succinate dehydrogenase (Complex II)} + \text{fumarase} \\ &+ \text{malate dehydrogenase 2}\end{aligned}$$

Reduced metabolic flexibility, defined as the ability to modulate between fatty acid and glucose oxidation in response to feeding or insulin stimulation (Kelley and Mandarino, 2000), is quantified in clinical research by examining changes in the respiratory quotient (RQ), which reflects the ratio of carbon dioxide produced relative to the oxygen consumed (**Eq. 4**).

Eq. 4:

$$RQ = \frac{\text{CO}_2 \text{ production}}{\text{O}_2 \text{ consumption}}$$

To determine whether experimental disruption in flux for a metabolic reaction causes changes in these characteristic metabolic phenotypes, we compared phenotypic scores from each KD to the corresponding phenotypic score from the normal (control) score. Since ATP+Cr-P production are closely linked in muscle, we summed these high-energy phosphate molecules to simplify the analysis (ATP+Cr-P). Thus, we assessed the ratio

of KD to control for the ATP+Cr-P-production and cumulative-TCA-flux phenotypes (**Eq. 5 and 6**):

Eq. 5:

$$ATP+Cr-P \ ratio = \frac{\sum (KD \ ATP+Cr-P \ production)}{\sum (Control \ ATP+Cr-p \ production)}$$

Eq. 6:

$$TCA \ ratio = \frac{\sum KD \ TCA \ flux}{\sum Control \ TCA \ Flux}$$

In normal metabolism, RQ (**Eq. 4**) increases as the individual shifts from fatty acid oxidation in the fasting state to glucose oxidation in the fed state (Kelley and Mandarino, 2000). In contrast to healthy, insulin sensitive individuals, insulin resistant and obese individuals have (1) higher fasting RQ and (2) lower fed RQ. Since both of the above phenotypes need to be true to indicate metabolic inflexibility, we thus define it as a logical, binary equation (**Eq. 7**):

Eq. 7:

$$\text{metabolic inflexibility} = (KD \ RQ_{fast} > Control \ RQ_{fast}) \text{ AND } (KD \ RQ_{fed} < Control \ RQ_{fed})$$

If **Eq. 7** is true, we then assess the magnitude of difference between fasted and fed RQ values: a greater difference indicates decreased flexibility/increased inflexibility (**Eq. 8**).

Eq. 8:

$$\text{Metabolic inflexibility score} = \text{IF} (\text{metabolic inflexibility} = \text{TRUE}),$$

```
then  $\Sigma(|KD\ RQfast - Control\ RQfast| + |KD\ RQfed - Control\ RQfed|)$   
else 0
```

Ratios less than one for either ATP+Cr-P production (**Eq. 5**) or cumulative TCA flux (**Eq. 6**) and any non-zero score for metabolic flexibility (**Eq. 8**) are considered to reflect insulin resistance phenotypes.

Pathway Analysis

We assigned each of the 388 model reactions to a KEGG pathway(s) based on its EC number, or if none were available, we assigned one manually. We also created pathways including reactions utilizing common energy metabolites (e.g. creatine, nicotinamide adenine dinucleotide (NAD), and flavin adenine dinucleotide (FAD)) and defined a cytosolic-mitochondrial NADH shuttle pathway. Finally, an “All Reactions Pathway,” containing all 388 reactions in the model, was used as the background distribution. The 47 pathways in our model are delineated in **Supplemental File All KDs-fluxes, scores, and p-values.xls, pathways tab**. We then used the Fisher’s exact test to determine if any of the pathways was significantly enriched in modulating the three metabolic phenotypes in any of the 3 states (fasted, mixed, fed) or four nutrient conditions—i.e., whether the number of perturbations in a specific pathway that alter the phenotype is greater than expected by chance. To account for multiple-hypothesis testing, we used the Benjamini-Hochberg method to calculate false discovery rate (FDR).

***In Silico* Modeling Assumptions**

In addition to assumptions made with the FBA model (Oberhardt et al., 2009), we add three additional assumptions. First, our model assumes that necessary hormones and enzymes are in place to seamlessly modulate fuel metabolism, between fatty acid and glucose metabolism. Secondly, because the flux into muscle of all lipid and amino acid species is unknown, we assume the uptake flux is proportional to plasma concentrations (Cynober, 2002; MacLaren et al., 2000). Finally, we assume the system reaches a steady state over enough time to maintain constant flux, and that concentrations of substrates in plasma will be stably maintained over time.

Primary Cell Isolation and Culture

All leg muscles were isolated from 4-week-old PDK2/4 KO mice (Jeoung and Harris, 2007) and wild type control mice by digesting with 2.4 U/mL dispase and 1% collagenase. Cells were grown in F10 medium supplemented with 20% fetal bovine serum and penicillin/streptomycin, with 2.5 ng/mL basic fibroblast growth factor added daily. Myoblasts were selected for by differential plating upon collagen-coated dishes for successive passages until cultures were over 97% pure, approximately 4 passages.

siRNA Transfection

We used specific siRNA oligonucleotides against ETFDH (ON-TARGETplus SMARTpool; Dharmacon - Thermo Fisher Scientific, Rockford, IL, USA) or a scrambled control that were transfected overnight using HiPerFect (Qiagen, Valencia, CA), based

on manufacturer's instructions. Myocytes were used 72 hours after transfection for analyses of knockdown efficiency and functional readouts.

qRT-PCR Analysis

Total RNA was extracted 72 hours post-KD by using RiboZol reagent (AMRESCO, Solon, OH, USA). For quantitative mRNA analysis, 1 µg of total RNA was reverse-transcribed with High Capacity cDNA Reverse Transcription Kit (Life Technologies). The cDNA reaction was subjected to quantitative real-time PCR analysis using iTaq Universal SYBR Green Supermix (Bio-Rad, Hercules, CA, USA) and ABI 7900HT Real-Time PCR System (Life Technologies), following the manufacturer's instructions. GAPDH and 36B4 were used as internal housekeeping genes. Relative gene expression was calculated by the $2^{-\Delta\Delta CT}$ method.

Western Blot Analysis

At 72 hours post KD, total protein was obtained by lysis with 1% sodium dodecyl sulfate in phosphate-buffered saline (PBS). Protein concentrations were determined with a bicinchoninic acid assay (BCA; Pierce – Thermo Fisher Scientific). Equal amounts of protein were run on a 10% SDS-PAGE gel and transferred to nitrocellulose. Membranes were blocked in 5% milk for one hour and then incubated with primary antibodies as indicated. Specific secondary antibodies and enhanced chemiluminescence reagents were used to visualize bands.

Adenosine Nucleotide Measurements

Levels of adenine nucleotides were measured by a coupled enzymatic assay (Detimary et al., 1995). Cells were grown in an opaque 96-well plate with clear bottom. Cells were washed twice in PBS, then put in KRB buffer with 5.5 mM glucose for 1 hr. Next, 100 μ l of the CellTiter-Glo luminescent assay reagent (Promega, Fitchburg, WI, USA) was added and incubated for 15 min. Luminescence was read using a multiplate reader. Untreated wells were used to determine relative protein content by BCA assay to normalize the data.

Citrate Synthase Activity Assay

Citrate synthase (CS) activity was determined using an enzymatic method based on a commercially available assay kit (CS0720 Sigma, St. Louis, MO, USA). Cells were lysed in RIPA buffer and added to a 96 well plate. Assay buffer (100 mM Tris pH 7.5) with 300 nM Acetyl-CoA and 100 nM DTNB (5,5'-dithiobis-(2-nitrobenzoic acid) was added to all wells. Plate was read at 412 nm for 1.5 mins, with a read every 10 seconds to determine endogenous CS activity. The curve slope was used to calculate the enzymatic activity, a BCA assay was used to normalize the data per milligram of protein.

Substrate Utilization Analysis

Cellular respiration was assessed using a Seahorse XF24 Flux Analyzer. Cells were treated overnight with 250 μ M palmitate in 0.1 % BSA. The following day, cells were washed twice in PBS, and then incubated in KR buffer with 5.5 mM glucose and 250 μ M palmitate in 0.1% BSA for 1 hr. Resting oxygen consumption rate (OCR) and

extracellular acidification rate (ECAR) were measured 4 times over a period of 20 mins. Then, 5.5 mM glucose was injected into each well, and the OCR and ECAR were measured 4 times over 20 mins. After the assay, total DNA was isolated using 50 mM NaOH and quantified with a spectrophotometer for normalization of results.